Coordination chemistry of new selective ethylene trimerisation ligand $Ph_2PN(^iPr)P(Ph)NH(R)$ (R = ^{i}Pr, Et) and tests in catalysis†‡

Bhaskar Reddy Aluri,[a] Normen Peulecke,[a] Stephan Peitz,[a] Anke Spannenberg,[a] Bernd H. Müller,[a] Stefan Schulz,[a] Hans-Joachim Drexler,[a] Detlef Heller,[a] Mohammed H. Al-Hazmi,[b] Fuad M. Mosa,[b] Anina Wöhl,[c] Wolfgang Müller[c] and Uwe Rosenthal*[a]

Received 7th May 2010, Accepted 28th May 2010
First published as an Advance Article on the web 30th July 2010
DOI: 10.1039/c0dt00440e

The synthesis of [$Ph_2PN(^iPr)P(Ph)NH(R)$] (R = ^{i}Pr, Et) (**1**, **2**) is described and the structure of **2** has been determined by single-crystal X-ray analysis. Compound **1** readily reacts with chromium(0), nickel(0), nickel(II), palladium(II), platinum(II) and iron(II) complexes to give four-membered rings (**3–10**) *via* P,P′ coordination. The molecular structures of [$Cr(CO)_4${$Ph_2PN(^iPr)P(Ph)NH(R)$-*P*,*P*′}] (R = ^{i}Pr, Et) (**3**, **4**), [$Cr(CO)_3(NCCH_3)${$Ph_2PN(^iPr)P(Ph)NH(^iPr)$-*P*,*P*′}] (**5**), [Ni{$Ph_2PN(^iPr)P(Ph)NH(^iPr)$-*P*,*P*′}$_2$] (**6**), *cis*-[$MX_2${$Ph_2PN(^iPr)P(Ph)NH(^iPr)$-*P*,*P*′}] (M = Ni, Pd, Pt; X = Cl or Br) (**7**, **8**, **9**) and *trans*-[$Fe(NCCH_3)_2${$Ph_2PN(^iPr)P(Ph)NH(^iPr)$-*P*,*P*′}$_2$]$(BF_4)_2$ (**10**) have been determined by X-ray diffraction. In the solid state, these complexes show tight phosphine bite angles in the range 67.89(2)° to 74.97(4)° and the central nitrogen atom adopts an almost planar (sp^2) geometry. Complexes **3**, **5**, **6**, **7** and **10** are tested for their catalytic activity in ethylene oligomerisation. Additionally, complex **10** is tested in hydrogenation of olefins.

Introduction

Organometallic complexes containing functionalized phosphine and aminophosphine ligands have attracted considerable interest in recent years, due to their wide spread application potential in the field of catalysis.[1] In addition, some aminophosphines and derivatives have also been investigated as anticancer drugs,[2] herbicides and antimicrobial agents, as well as neuroactive agents.[3] Functionalized aminophosphines are proved to be versatile ligands since the functional group can be modified to tune the chemical and physical properties of the final product, resulting in significant changes in their coordination behaviour, in the structural parameters of the resulting complexes and in their subsequent reactivity.[4]

We have an ongoing interest in such compounds[5] and very recently, we reported the synthesis of an aminophosphine ligand type $Ph_2PN(R)P(Ph)NH(R)$ (R ≠ H) (PNPNH)[6] which is related to the well known bis(diphenylphosphino)-amines (PNP) and possesses an extra terminal NH function. Coordination of PNPNH to metal centres can occur through the lone pair of electrons at one or both of the phosphorus centres as well as by deprotonation of the NH group to form a tridentate ligand. The PNPNH compound $Ph_2PN(^iPr)P(Ph)NH(^iPr)$ **1** in conjunction with chromium is proved to be highly active in ethylene trimerisation by giving high yield and selectivity towards 1-hexene,[6a] comparable to Sasol's PNP ligand.

To further develop our understanding of this unique ligand system (PNPNH), we herein describe the synthesis and structural characterization of [$Ph_2PN(^iPr)P(Ph)NH(R)$] (R = ^{i}Pr, Et) (**1**, **2**), and also demonstrate that chromium(0), nickel(0), nickel(II), palladium(II), platinum(II) and iron(II) chelate complexes (**3–10**) can be readily prepared with these ligands. The newly synthesized chromium, nickel and iron complexes are tested in ethylene oligomerisation catalysis. Further, the iron complex is also tested in hydrogenation of simple olefins.

Results and discussion

The two different methods for the synthesis of PNPNH compounds were described earlier.[6a] Compound **1** was already known and prepared following the reported procedure. The reaction of $Ph_2PN(^iPr)PPhCl$[7] with a 1 : 1 mixture of $EtNH_2$ and toluene gave compound **2**. Workup of the reaction mixture, followed by recrystallization of the resulting residue from n-hexane gave **2** in a moderate yield (55%) as an air-stable, crystalline white solid readily soluble in diethyl ether, toluene, and methylene chloride. (Scheme 1). The $^{31}P\{^1H\}$ NMR spectra showed two broad singlets at δ 41.0 and 72.6 corresponding to two phosphorus nuclei with different chemical environments.

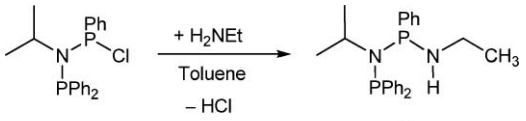

2

Scheme 1 Synthesis of $Ph_2PN(^iPr)P(Ph)NH(Et)$ (**2**).

[a]*Leibniz-Institut für Katalyse e. V. an der Universität Rostock, Albert-Einstein-Straße 29a, 18059, Rostock, Germany. E-mail: uwe.rosenthal@catalysis.de*
[b]*Saudi Basic Industries Corporation, P.O. Box 42503, Riyadh, 11551, Saudi Arabia*
[c]*Linde AG, Linde Engineering Division, Dr -Carl-von-Linde-Straße 6-14, 82049, Pullach, Germany*

† CCDC reference numbers 780221–780229. For crystallographic data in CIF or other electronic format see DOI: 10.1039/c0dt00440e

‡ Dedicated to Professor Sandro Gambarotta on the occasion of his 60th birthday.

Crystals suitable for X-ray analysis were obtained from a saturated n-hexane solution of **2** at –40 °C. Crystal data and some details of the data collection and refinement of the ligand and prepared complexes (*vide infra*) are given in Table 1. The molecular structure of compound **2** and selected bond distances and angles are given in Fig. 1. The N1 atom is in a slightly distorted trigonal planar environment with the angles adding up to 359.8° (P1–N1–C19 116.61(11), P2–N1–C19 120.09(12), P1–N1–P2 123.09(8)°) and the P2 atom is in a distorted trigonal pyramidal shape with angles ranging from 99.75(8)° to 107.70(8)°, the median value being 100.01(7). The P–N–P, N–P–N angles and P–N distances are in the usual range and are comparable to the earlier reported compound **1**.[6]

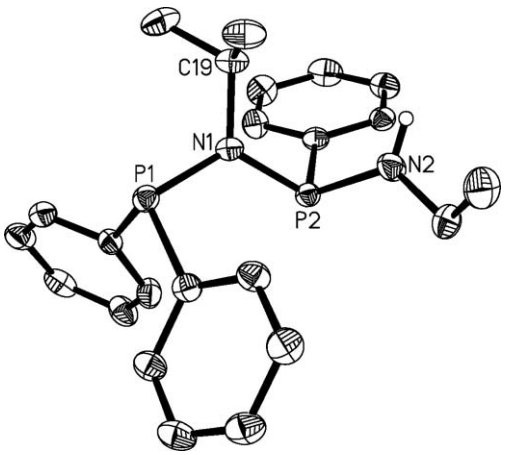

Fig. 1 Molecular structure of $Ph_2PN(^iPr)P(Ph)NH(Et)$ (**2**). Thermal ellipsoids are drawn at the 30% probability level. All the H atoms except the one attached to the N2 atom are omitted for clarity. Important bond lengths [Å] and angles [°]: N1–P1 1.7092(15), N2–P2 1.678(2), N1–P2 1.7155(14), P1–N1–P2 123.09(8), N2–P2–N1 107.70(8).

Our previous publication[6a] describes a very interesting coordination behaviour of ligand **1** which coordinates with chromium and aluminium centres in either a *P*,*P*′ or *P*,*N* chelation mode. To gain more knowledge about the coordination chemistry of this ligand, the chromium tetracarbonyl complexes $[Ph_2PN(^iPr)P(Ph)N(R)H]Cr(CO)_4$ (R = ^{i}Pr, Et) (**3**, **4**) were prepared (Scheme 2) following the method reported by Wass *et al.*[8] Reaction of **1** or **2** with $Cr(CO)_6$ in toluene at reflux temperature furnished chromium(0) carbonyl complexes **3** and **4** by CO displacement with diphosphine, in a moderate yield (60% and 55%). Spectroscopic data are consistent with a (*P*,*P*′)-κ² coordination mode.

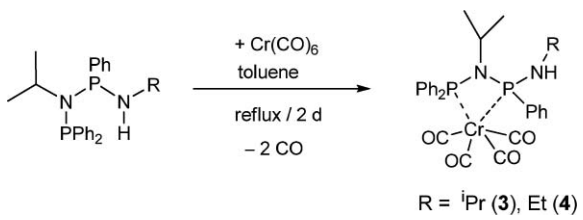

Scheme 2 Synthesis of $[Cr(CO)_4\{Ph_2PN(^iPr)P(Ph)NH(R)$-*P*,*P*′$\}]$ (R = ^{i}Pr, Et) (**3**, **4**).

The infrared spectra of **3** and **4** reveal very similar stretching frequencies and are consistent with those previously reported for *cis*-phosphine-substituted tetracarbonyl complexes $Cr(CO)_4\{NMe(PPh_2)_2\}$[9] (~1925 cm^{-1}) and $Cr(CO)_4\{(Ph_2PCH_2PPh_2\}$[10] (~1927 cm^{-1}), and are tabulated in Table 2.

A single-crystal X-ray diffraction study confirmed the spectroscopic assignment of **3** and **4**. Single crystals were obtained from a dichloromethane–methanol solution at –40 °C. The structures and selected bond distances and angles are illustrated in Fig. 2 and 3. Both complexes **3** and **4** show distorted octahedral coordination at chromium with a nearly planar Cr–P–N–P ring. The sum of the angles around N1 is 359.3° and 359.9° respectively for **3** and **4**, and implies sp^2 hybridisation at this nitrogen. The Cr–CO bond lengths *trans* to the phosphorus atoms are slightly shorter than those *trans* to other carbonyls in **3** and are consistent with the weaker *trans*-influence of the Cr–P bond. The Cr–P bond lengths, P–Cr–P and P–N–P bond angles are similar to the ones reported for $[Cr(CO)_4\{Ar_2PN(Me)PAr_2\}]$.[8]

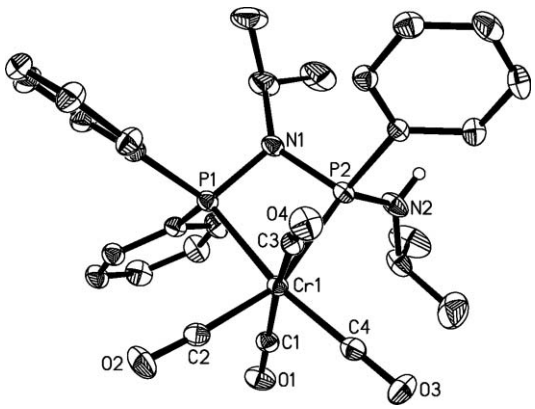

Fig. 2 Molecular structure of $[Cr(CO)_4\{Ph_2PN(^iPr)P(Ph)NH(^iPr)$-*P*,*P*′$\}]$ (**3**). Thermal ellipsoids are drawn at the 30% probability level. All the H atoms except the one attached to the N2 atom are omitted for clarity. Important bond lengths [Å] and angles [°]: N1–P1 1.695(2), N2–P2 1.646(2), N1–P2 1.715(2), P1–Cr1 2.3388(6), P2–Cr1 2.3602(6), Cr1–C1 1.877(2), Cr1–C2 1.852(2), Cr1–C3 1.879(2), Cr1–C4 1.856(2); P1–N1–P2 100.61(9), N2–P2–N1 112.27(10), P1–Cr1–P2 67.90(2).

Reaction of *fac*-$Cr(CO)_3(NCCH_3)_3$[11] with an equimolar quantity of **1** in acetonitrile at 60 °C results in the quantitative formation of $[Cr(CO)_3(NCCH_3)\ \{Ph_2PN(^iPr)P(Ph)NH(^iPr)$-*P*,*P*′$\}]$ (**5**) (Scheme 3). In the room temperature NMR spectra two sets of signals are observed in a 2 : 1 ratio belonging to two isomers. The $^{31}P\{^1H\}$ NMR signals appeared at 99.4, 121.7 (d, J = 16.7 Hz) and 107.0, 120.6 (d, J = 25.6 Hz) for *major* and *minor* isomers respectively. The infrared spectrum shows three carbonyl stretching vibrations at 1923, 1830, 1802 cm^{-1} and are comparable to the values reported for $[Mo(CO)_3(NCCH_3)\{Ph_2PN(^iPr)P(Ph)(DMP)$-*P*,*P*′$\}]$ (DMP = 3,5-dimethylpyrazole).[12]

Single crystals of **5** suitable for X-ray diffraction were obtained from a saturated solution of acetonitrile at –20 °C. The molecular structure and selected bond distances and angles are illustrated in Fig. 4. Complex **5** is a six-coordinated complex with a *P*,*P*′-bidentate [PNPNH] ligand with a spectating amine but coordinated CH_3CN. It is stable in pure and dry CH_3CN, and traces of moisture in solvent led to the formation of substantial

Table 1 Crystallographic data

Compd	**2**	**3**	**4**	**5**	**6**	**7**	**8**	**9**	**10**
Empirical formula	$C_{23}H_{28}N_2P_2$	$C_{28}H_{30}CrN_2O_4P_2$	$C_{27}H_{28}CrN_2O_4P_2$	$C_{29}H_{33}CrN_3O_3P_2$	$C_{48}H_{60}N_4NiP_4$ (0.5 C_6H_{14})	$C_{24}H_{30}Cl_2N_2NiP_2$ (CH_2Cl_2)	$C_{24}H_{30}Cl_2N_2P_2Pd$	$C_{24}H_{30}Br_2N_2P_2Pt$ (0.5 CH_2Cl_2)	$C_{52}H_{66}B_2F_8FeN_6P_4$
Formula weight	394.41	572.48	558.45	585.52	918.68	622.98	585.74	805.81	1128.46
T/K	200(2)	200(2)	200(2)	200(2)	200(2)	200(2)	200(2)	200(2)	200(2)
Cryst. syst.	Orthorhombic	Orthorhombic	Monoclinic	Orthorhombic	Triclinic	Triclinic	Monoclinic	Monoclinic	Monoclinic
Space group	$P2_12_12_1$	*Pbca*	$P2_1/c$	*Pbca*	$P\bar{1}$	$P\bar{1}$	$P2_1/c$	$P2_1/n$	$P2_1/c$
a/Å	8.902(2)	15.5122(10)	11.262(2)	12.7627(2)	10.8037(6)	8.5768(2)	8.7588(3)	9.4775(2)	20.804(4)
b/Å	9.978(2)	17.7614(12)	14.220(3)	17.6292(3)	11.7151(6)	18.4703(5)	14.6095(3)	13.2311(2)	13.105(3)
c/Å	24.459(5)	21.5240(14)	17.443(4)	26.0903(5)	21.2583(10)	18.9358(5)	20.0055(6)	22.4851(5)	20.917(4)
α (°)	90	90	90	90	89.596(4)	97.413(2)	90	90	90
β (°)	90	90	102.91(3)	90	87.817(4)	91.558(2)	90.028(2)	101.4274(17)	103.96(3)
γ (°)	90	90	90	90	69.521(4)	96.707(2)	90	90	90
V/Å^3	2172.5(8)	5930.3(7)	2723.0(9)	5870.2(2)	2518.7(2)	2951.58(13)	2559.94(13)	2763.68(10)	5534.2(19)
Z	4	8	4	8	2	4	4	4	4
μ/mm^{-1}	0.210	0.527	0.572	0.533	0.549	1.145	1.073	8.198	0.456
Crystal size/mm	0.45 × 0.40 × 0.35	0.30 × 0.25 × 0.15	0.35 × 0.25 × 0.22	0.3 × 0.2 × 0.2	0.30 × 0.23 × 0.20	0.45 × 0.35 × 0.27	0.35 × 0.30 × 0.06	0.30 × 0.11 × 0.06	0.40 × 0.30 × 0.30
No. of rflns (measd)	28706	5827	44916	108511	30124	49081	37483	42678	9746
No. of rflns (indep)	4279	5827	6262	7917	9886	13536	5879	6342	9746
No. of parameters	248	338	329	352	547	589	288	315	610
Final R indices [$I > 2\sigma(I)$]	$R_1 = 0.0297$, w$R_2 = 0.0664$	$R_1 = 0.0321$, w$R_2 = 0.0568$	$R_1 = 0.0291$, w$R_2 = 0.0794$	$R_1 = 0.0356$, w$R_2 = 0.0827$	$R_1 = 0.0371$, w$R_2 = 0.0679$	$R_1 = 0.0314$, w$R_2 = 0.0709$	$R_1 = 0.0266$, w$R_2 = 0.0555$	$R_1 = 0.0232$, w$R_2 = 0.0393$	$R_1 = 0.0462$, w$R_2 = 0.0660$
R indices (all data)	$R_1 = 0.0352$, w$R_2 = 0.0677$	$R_1 = 0.0608$, w$R_2 = 0.0605$	$R_1 = 0.0374$, w$R_2 = 0.0815$	$R_1 = 0.0562$, w$R_2 = 0.0877$	$R_1 = 0.0813$, w$R_2 = 0.0739$	$R_1 = 0.0515$, w$R_2 = 0.0741$	$R_1 = 0.0395$, w$R_2 = 0.0578$	$R_1 = 0.0356$, w$R_2 = 0.0409$	$R_1 = 0.0807$, w$R_2 = 0.0681$
Largest diff. peak and hole/e Å^{-3}	0.232 and –0.180	0.311 and –0.209	0.320 and –0.358	0.432 and –0.443	0.382 and –0.230	1.080 and –0.860	0.472 and –0.403	1.047 and –1.066	1.069 and –0.968

Table 2 Carbonyl stretching frequencies for complexes **3** and **4**

	ν(CO) (CH_2Cl_2, cm^{-1})	$\nu(CO)_{av}$ (CH_2Cl_2, cm^{-1})
3	1870, 1896, 1918, 2005	1922
4	1877, 1890, 1917, 2005	1922

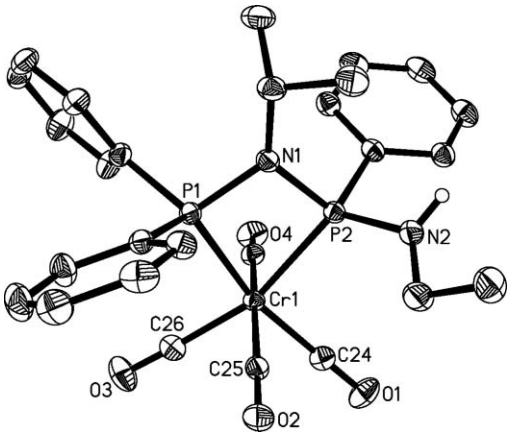

Fig. 3 Molecular structure of [$Cr(CO)_4${$Ph_2PN(^iPr)P(Ph)NH(Et)$-*P*,*P*′}] (**4**). Thermal ellipsoids are drawn at the 30% probability level. All the H atoms except the one attached to N2 atom are omitted for clarity. Important bond lengths [Å] and angles [°]: N1–P1 1.6958(13), N2–P2 1.6519(14), N1–P2 1.7131(13), P1–Cr1 2.3342(7), P2–Cr1 2.3312(6), Cr1–C25 1.865(2), Cr1–C26 1.863 (2), Cr1–C27 1.881(2), Cr1–C24 1.854(2); P1–N1–P2 100.15(7), N2–P2–N1 112.67(7), P1–Cr1–P2 68.16(2).

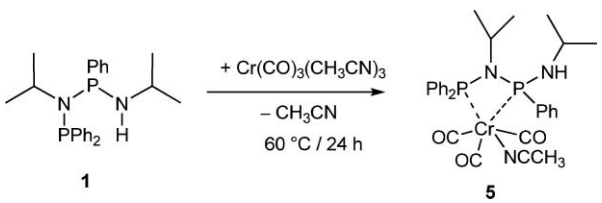

Scheme 3 Synthesis of [$Cr(CO)_3(NCCH_3)${$Ph_2PN(^iPr)P(Ph)NH(^iPr)$-*P*,*P*′}] (**5**).

quantities of tetracarbonyl complex **3** by redistribution. This kind of behaviour is observed earlier in molybdenum complexes.[12] In the solid state chromium possesses a distorted octahedral geometry with acetonitrile lying *trans* to a CO ligand and the remaining two carbonyls located *trans* to phosphorus atoms. The three Cr–CO distances are 1.853(2), 1.819(2), 1.855(2) where the shortest distance represents the carbonyl ligand located *trans* to the acetonitrile group. The P–N–P angle is the same as that observed for the tetracarbonyl complex **3**.

Further, the coordination chemistry of **1** with group 10 transition-metals (Ni, Pd and Pt) was explored. Treatment of $Ni(COD)_2$ with 2 equiv. of PNPNH (**1**) in n-hexane at ambient temperature afforded [Ni{$Ph_2PN(^iPr)P(Ph)NH(^iPr)$-*P*,*P*′}$_2$] (**6**) in 50% yield (Scheme 4).

As expected, in the $^{31}P\{^1H\}$ NMR spectrum two multiplets centered at δ 77.5, 98.5 are observed for this bis-chelate complex **6** due to coupling of each phosphorus with three other phosphorus nuclei and possible rotation around the metal center in the solution

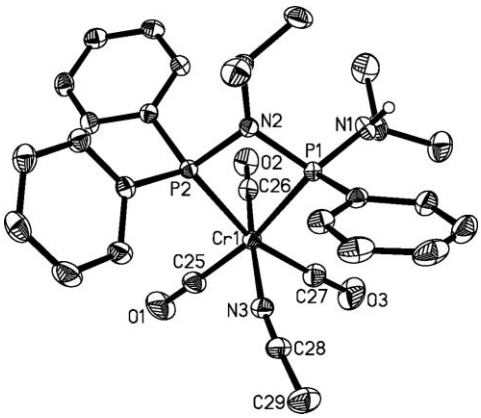

Fig. 4 Molecular structure of [$Cr(CO)_3(NCCH_3)${$Ph_2PN(^iPr)$–P(Ph)NH(^{i}Pr)-*P*,*P*′}] (**5**). Thermal ellipsoids are drawn at the 30% probability level. All the H atoms except the one attached to N1 atom are omitted for clarity. Important bond lengths [Å] and angles [°]: N2–P2 1.6973(14), N1–P1 1.6432(15), N2–P1 1.7270(13), P2–Cr1 2.3455(5), P1–Cr1 2.3637(5), Cr1–C25 1.853(2), Cr1–C26 1.819(2), Cr1–C27 1.855(2), Cr1–N3 2.0531(15); P1–N2–P2 100.73(7), N2–P1–N1 113.13(7), P1–Cr1–P2 68.113(15).

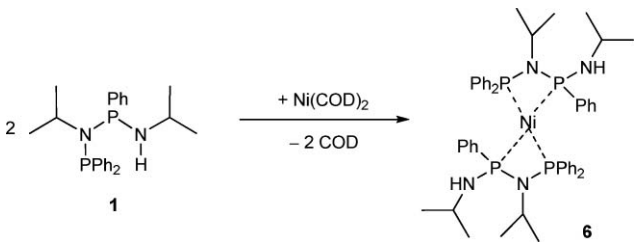

Scheme 4 Synthesis of [Ni{$Ph_2PN(^iPr)P(Ph)NH(^iPr)$-*P*,*P*′}$_2$] (**6**).

state. Apart from it, in ^{1}H NMR two sets of signals in 7 : 3 ratio (possibly two different isomers) are observed in the aliphatic region while the aryl region is less informative. Owing to the adjacent chiral phosphorus atom all the (eight) methyl protons show different resonances. Among these, two methyl resonances are strongly upfield shifted (0.03 and 0.17 ppm) indicating that these methyl groups are shielded by the phenyl groups. The more preferable isomeric structure is further characterized by X-ray crystal structure analysis.

Crystals of **6** suitable for X-ray analysis were obtained from a saturated n-hexane solution at –40 °C. The molecular structure is shown in Fig. 5. The crystal structure shows one molecule of **6** and a half n-hexane molecule in the asymmetric unit. The nickel atom adopts a distorted tetrahedral geometry. The planes defined by P1–N1–P2–Ni1 and P3–N3–P4–Ni1 are nearly perpendicular to each other. The angle between these two planes is 87.12(3). The P–Ni bond distances and P–Ni–P angles are in the range reported for the bis-chelate nickel(0) complex [Ni{$Ar_2PN(Me)PAr_2$}$_2$].[13]

The reaction of **1** with group 10 metals *i.e.* $NiCl_2$(DME), $PdCl_2(PhCN)_2$ and $PtBr_2$(COD) in a 1 : 1 molar ratio at room temperature affords air stable, mononuclear, square planar complexes *cis*-[$NiCl_2${$Ph_2PN(^iPr)P(Ph)NH(^iPr)$-*P*,*P*′}] (**7**), *cis*-[$PdCl_2${$Ph_2PN(^iPr)P(Ph)NH(^iPr)$-*P*,*P*′}] (**8**), *cis*-[$PtBr_2${$Ph_2PN(^iPr)P(Ph)NH(^iPr)$-*P*,*P*′}] (**9**) (Scheme 5) in excellent yields

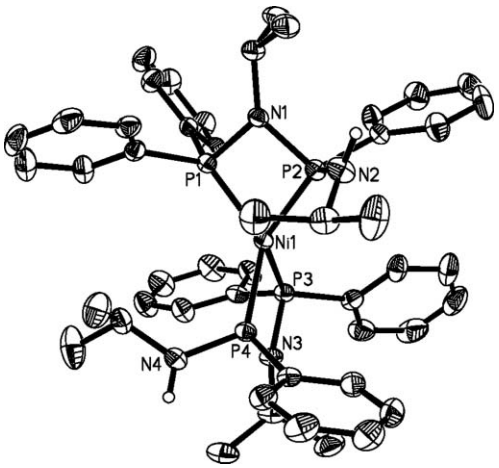

Fig. 5 Molecular structure of [Ni{$Ph_2PN(^iPr)P(Ph)NH(^iPr)$-*P*,*P*′}$_2$] (**6**). Thermal ellipsoids are drawn at the 30% probability level. All the H atoms except the one attached to the N2 atom are omitted for clarity. Important bond lengths [Å] and angles [°]: N1–P1 1.710(2), N2–P2 1.674(2), N1–P2 1.729(2), N3–P3 1.707(2), N4–P4 1.668(2), N3–P4 1.723(2), P1–Ni1 2.1590(8), P2–Ni1 2.1573(8), P3–Ni1 2.1603(8), P4–Ni1 2.1558(8), P1–N1–P2 99.54(11), N2–P2–N1 110.18(12), P3–N3–P4 99.49(11), N4–P4–N3 109.79(12), P1–Ni1–P2 74.93(3), P2–Ni1–P3 130.64(3), P3–Ni1–P4 74.68(3), P4–Ni1–P1 130.35(3).

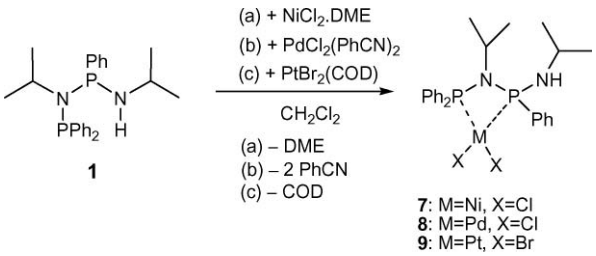

Scheme 5 Synthesis of *cis*-[MX_2{$Ph_2PN(^iPr)P(Ph)NH(^iPr)$-*P*,*P*′}] (M = Ni, Pd, Pt; X = Cl or Br) (**7**, **8**, **9**).

(80–89%). These complexes are insoluble in benzene and toluene, partially soluble in THF but are readily soluble in CH_2Cl_2.

The room temperature $^{31}P\{^1H\}$ NMR spectra of **7**, **8**, and **9** in CD_2Cl_2 display two doublets at δ 41.9, 44.1 ($^2J_{PP}$ = 180.5 Hz); 35.5, 36.7 ($^2J_{PP}$ = 21.2 Hz); and 16.3, 17.9 ($^2J_{PP}$ = 35.0 Hz, $^1J_{PtP}$ = 3600, 3402 Hz) ppm, respectively. The large $^1J_{PtP}$ coupling constant observed for **9** is in good agreement with a *cis* disposition of ligands (*i.e.* phosphorus *trans* to chloride). The $^{31}P\{^1H\}$ NMR spectra of the complexes shows an AB pattern and the chemical shifts are shifted considerably upfield compared with the free ligand. This shift indicates that the ligand is coordinated in a *P*,*P*′-chelating mode, forming four-membered metallacycles,[14] as has been shown by the X-ray crystal structure determination of **7**, **8** and **9**. It is well known that the shielding of the coordinated $\rangle$P–N ($\Delta\delta$) depends on the electronegativity of the substituents attached to the phosphorus centre and decreases in the order NCP–N > CCP–N.[15] Among these complexes (**7–9**) the central phosphorus (NCP–N) shows the highest shielding ($\Delta\delta$ = −24 to −50 ppm), relative to the terminal phosphorus (Ph_2P–N) ($\Delta\delta$ = +0.7 to −25 ppm). This shielding effect is increased in the order Ni < Pd < Pt. Similar types of shielding effect are observed in diphosphazane[4] and diphosphinoalkane[16] complexes. Additionally, the presence of a four-membered ring may also have some influence on the observed high shielding. In the ^{1}H NMR spectrum four different methyl(^{i}Pr) resonances are observed owing to the presence of an adjacent phosphorus chiral centre. From these methyl resonances two are shielded and the other two are deshielded compared to the free ligand chemical shifts. The sharp signals in ^{1}H, and $^{31}P\{^1H\}$ NMR spectra of **7** are consistent with a diamagnetic square-planar Ni species in solution.

Single crystals of **7**, **8** and **9** suitable for X-ray diffraction studies were obtained by slow diffusion of diethyl ether into a solution of the complexes in dichloromethane at room temperature. A perspective view of the molecules with important bond lengths and angles is given in Fig. 6–8.

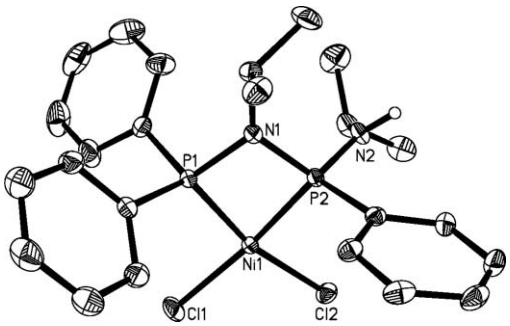

Fig. 6 Molecular structure of [$NiCl_2${$Ph_2PN(^iPr)P(Ph)NH(^iPr)$-*P*,*P*′}] (**7**). Only one of the two molecules of the asymmetric unit is shown. Thermal ellipsoids are drawn at the 30% probability level. All the H atoms except the one attached to N2 atom are omitted for clarity. Important bond lengths [Å] and angles [°]: N1–P1 1.687(2), N2–P2 1.620(2), N1–P2 1.699(2), P1–Ni1 2.1108(6), P2–Ni1 2.1220(6), Ni1–Cl1 2.2010(6), Ni1–Cl2 2.1787(6), P1–N1–P2 96.95(9), N2–P2–N1 115.07(10), P1–Ni1–P2 73.58(2), P2–N2–C16 96.95(9), Ni1–P2–N2 119.48(7), Cl1–Ni1–Cl2 96.91(3); N3–P3 1.686(2), N4–P4 1.630(2), N3–P4 1.694(2), P3–Ni2 2.1152(6), P4–Ni2 1.2342(5), Ni2–Cl3 2.1843(6), Ni2–Cl4 2.2058(6), P3–N3–P4 97.88(9), N4–P4–N3 114.62(9), P3–Ni2–P4 73.71(2), P4–N4–C40 124.62(14), Ni2–P4–N4 116.25(7), Cl3–Ni2–Cl4 97.52(3).

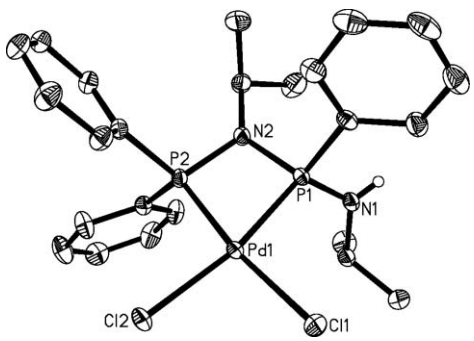

Fig. 7 Molecular structure of [$PdCl_2${$Ph_2PN(^iPr)P(Ph)NH(^iPr)$-*P*,*P*′}] (**8**). Thermal ellipsoids are drawn at the 30% probability level. All the H atoms except the one attached to N1 atom are omitted for clarity. Important bond lengths [Å] and angles [°]: N2–P2 1.688(2), N1–P1 1.618(2), N2–P1 1.704(2), P2–Pd1 2.2007(5), P1–Pd1 2.2237(4), Pd1–Cl2 2.3663(5), Pd1–Cl1 2.3539(6), P1–N2–P2 99.87(9), N2–P1–N1 114.40(10), P1–Pd1–P2 71.84(2).

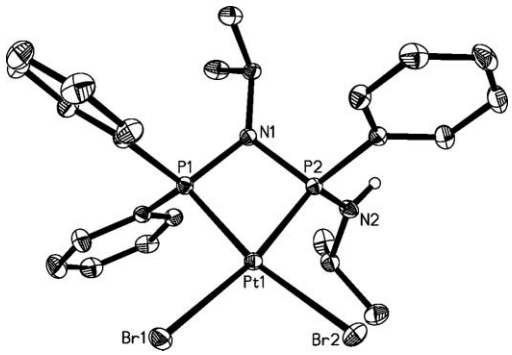

Fig. 8 Molecular structure of [$PtBr_2${$Ph_2PN(^iPr)P(Ph)NH(^iPr)$-*P*,*P*′}] (**9**). Thermal ellipsoids are drawn at the 30% probability level. All the H atoms except the one attached to the N2 atom are omitted for clarity. Important bond lengths [Å] and angles [°]: N1–P1 1.695(3), N2–P2 1.623(3), N1–P2 1.708(3), P1–Pt1 2.2084(8), P2–Pt1 2.2035(8), Pt1–Br1 2.4902(4), Pt1–Br2 2.4805(4), P1–N1–P2 100.14(14), N2–P2–N1 113.87(15), P1–Pt1–P2 72.54(3).

The solid-state structure of **7** shows the presence of two enantiomers (*R* and *S*) in the asymmetric unit along with two molecules of dichloromethane. The two enantiomers adopt a similar (but not identical) conformation. The geometry at the nickel centre is distorted square planar. The main distortions are the acute P1–Ni1–P2 (73.58(2)°), P3–Ni2–P4 (73.71(2)°) angles which results from the small bite angle of the ligand. Similar to the nickel complex, the molecules **8** and **9** (Fig. 7, 8) adopt a distorted square planar geometry at palladium and platinum with *cis*-halides and both phosphorus of the neutral ligand coordinated to the metal. The relative configuration of the asymmetric phosphorus atom in the depicted ligands is *S*. The *R* enantiomer is generated by the inversion symmetry of the space group. In addition, the asymmetric unit of **9** contains besides one complex molecule, a half CH_2Cl_2 as lattice solvent. Within the ligand, the P–N bond lengths are similar to those in the free ligand. The central nitrogen atom N1 (and N3 for **7**) adopts a planar geometry and the sum of the angles around the nitrogen is nearly 360°. The bite angles in **8** and **9** (71.845(3)° and 72.54(3)°) are relatively smaller compared to Ni(II) complex **7** (73.58(2)° and 73.71(2)°).

Finally, *trans*-[$Fe(CH_3CN)_2${$Ph_2PN(^iPr)P(Ph)NH(^iPr)$-*P*,*P*′}$_2$]-($BF_4$)$_2$ (**10**) was synthesized by the reaction of [$Fe(H_2O)_6$](BF_4)$_2$ with two equivalents of compound **1** in acetonitrile at room temperature (Scheme 6).

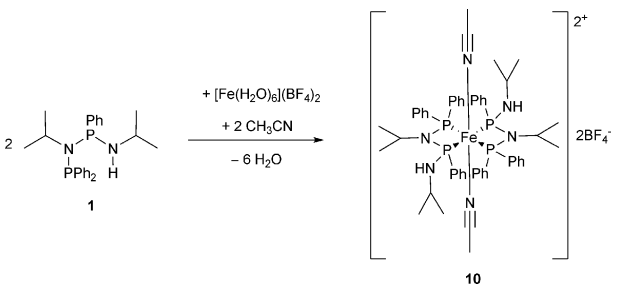

Scheme 6 Synthesis of *trans*-[$Fe(CH_3CN)_2${$Ph_2PN(^iPr)P(Ph)NH(^iPr)$-*P*,*P*′}$_2$]($BF_4$)$_2$ (**10**).

Similar to bis-chelate Ni(0) complex **6**, the room temperature $^{31}P\{^1H\}$ NMR spectra of **10** in CD_3CN display two multiplet signals which are centered at 91.6 and 105.4 ppm. The chemical shifts are deferred considerably downfield compared with the free ligand. In ^1H NMR two sets of signals are observed in a 2 : 1 ratio, belonging to two different isomers of complex **10**, probably formed by rotation of the PNPNH unit around the metal centre in solution. The major isomer is the one where two Ph_2P-groups are *trans* to each other and in the minor isomer they are *cis* to each other. The more preferable isomeric structure is further characterized by X-ray crystal structure analysis. Single crystals of **10** were obtained from an acetonitrile solution overlaying with MTBE (methyl ^{t}butyl ether) at room temperature. The asymmetric unit of **10** consists of two half molecules of the cation and two BF_4 anions. The molecular structure (Fig. 9) shows distorted octahedral coordination geometry at iron(II) with nearly planar Fe–P–N–P rings. The two molecules of acetonitrile are *trans* to each other and the PNPNH ligands coordinate in *P*,*P*′-chelating mode. The Fe–P bond distances and P–Fe–P bond angles are in the range of related iron(II) complexes.[17]

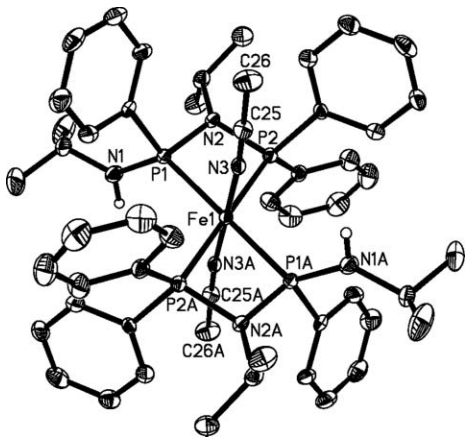

Fig. 9 Molecular structure of the cation [$Fe(CH_3CN)_2${$Ph_2PN(^iPr)$-P(Ph)$NH(^iPr)$-*P*,*P*′}$_2$]$^{+}$ of **10**$^{2+}$ (completed by using the symmetry operator −x + 2, −y, −z + 1). Thermal ellipsoids are drawn at the 30% probability level. All the H atoms except the ones attached to N1 and N1A, the second half cation of the asymmetric unit and the anions are omitted for clarity. Important bond lengths [Å] and angles [°]: N1–P1 1.657(3), N2–P1 1.709(3), N2–P2 1.706(3), Fe1–P1 2.2456(10), Fe1–P2 2.2701(12), P1–N2–P2 101.21(15), P1–Fe1–P2 71.52(4).

In all the above mentioned complexes (**3–10**), the nitrogen atoms were not involved in any coordination to the metal centres because the phosphorus atoms in the aminophosphine ligand are much stronger donor centres and thus, coordination to the metal centre takes place preferentially at the phosphorus atoms. However, it deserves to be noted that lithiation of compound **1**, followed by treatment with Li[$CpCrCl_3$] gave a *P*,*N*-coordinated Cr(III) complex.[6a]

Ethylene oligomerisation

As mentioned in the introduction, the PNPNH compound **1** forms a very efficient catalytic system in combination with $CrCl_3(THF)_3$ and triethylaluminium (TEA) for selective ethylene trimerisation, giving over 99% of 1-hexene in the fraction of the hexenes.[6a] In this context, it was interesting to check the activity of newly synthesized Cr(0) complexes in the ethylene

Table 3 Ethylene oligomerisation

Entry	Complex	C_2H_4 consumed/g	Productivity [d] (g g^{-1} M)	Activity (g g^{-1} M^d/h)	PE/g	Oligomer wt. (%) distribution				
						C4[e]	C6 (1-C6)	C8 (1-C8)	C10	C12+
1	**3**[a]	1.6	154	51	1.0	12	64 (84)	9 (50)	4	11
2	**3**[b]	6.0	577	289	0.8	5	86 (98)	2 (75)	4	3
3	**5**	4.6	442	221	0.6	27.2	54.7 (91)	6 (55)	2.8	9.3
4	**5**[b]	5.8	558	279	1.2	23.7	55.6 (92)	7.6 (68)	4.1	9
5	**6**	0	0	0						
6	**7**[c]	1.0	149	75	0	72	11.9 (75)	1.6	3.3	11.2
7	**10**	2.1	188	94	0	68	13 (54)	1.4 (36)	2	15.6

0.2 mmol complex, Al : Cr = 100, Toluene, 120 min run time, TEA as co-catalyst, 65 °C, 30 bar,[a] 180 min run time; [b] Activated for 30 min with UV light; [c] 0.05 mmol complex used; [d] M = Cr/Ni/Fe; [e] wt% of dissolved C4 only.

oligomerisation reaction which allows us to draw a comparison between the activities of Cr(III) and Cr(0) (Table 3). Complex **3** showed poor activity and furnished predominantly polyethene (PE) when TEA was used as activator and scavenger for CO (entry 1). Treatment of **3** with TEA in the presence of 10 mol% free ligand **1** followed by UV photolysis (30 min) gave active trimerisation catalyst (entry 2). The active species formed during photolysis might be stabilized by coordinating with added free ligand or TEA. This shows that photolysis of Cr(0) leads to an active catalyst system giving higher productivities compared to the non photolyzed reaction. About the active species of trimerisation catalysts one can only speculate. We have presented a possible active coordination motif before.[6a] Noteworthy in the case of the Cr(I) compound $[\{Cr(CO)_4(Ph_2PN(^iPr)PPh_2)\}\{Al\{OC(CF_3)_3\}_4\}]$ photolysis leads to catalyst degradation forming Cr(0) resulting in lower productivities.[18] The introduction of CH_3CN into the coordination sphere enhances the activity dramatically. Complex **5** treated with TEA alone (without activation by photolysis) shows four fold activity compared to the tetracarbonyl complex **3** (entries 1 and 3). Interestingly, selectivity towards 1-hexene is prevailed while a significant increase in the PE formation is observed compared to $CrCl_3(THF)_3$ system.[6] Contrary to this, introduction of acetonitrile in the $CrCl_3(Ph_2PN(Cy)PPh_2)$ system drastically changes the selectivity giving exclusively PE.[19] Activation of complex **5** with UV light has only a very little effect on activity and oligomer distribution, while a two fold increase in PE formation is observed (entries 3 and 4). The bis-chelate nickel(0) complex **6** did not show any activity under these conditions (entry 5). Complexes **7** and **10** did not produce any PE but the activity is considerably low (entry 6 and 7).

Hydrogenation

Iron(II) hydride complexes with diphosphine ligands and pendant amine bases show a rapid intramolecular exchange between the protonated base of a PNP-ligand and the hydride ligand. Here the amine group works as a proton acceptor in the heterolytic hydrogen activation.[20] With this concept in mind, it is tempting to test the iron complex **10** in hydrogenation of olefins.[21] The hydrogenation of cyclohexene and norbornadiene with **10** in 1,2-dichloroethane and THF did not show any consumption of hydrogen, even after addition of an external base (Et_3N). Working at a high pressure of hydrogen (56 bar) in the presence of cyclohexene and norbornadiene also gave no fruitful results.

Conclusion

Several transition metal complexes of new aminophosphine compounds **1** and **2** have been prepared which are relevant to ethylene oligomerisation. From these complexes (**3–10**) it becomes clear that these novel aminophosphine ligands have a pronounced tendency to form stable four-membered chelates. The terminal secondary amine is not involved in complexation with any of these metals and typically acts as a spectator group. However, the deprotonation of this terminal nitrogen occurs in the presence of alkylating agents such as TEA to give active catalysts for ethylene oligomerisation. While labile the acetonitrile coordinated chromium tricarbonyl complex can be activated by using TEA alone, the chromium tetracarbonyl complexes are activated only by photolysis in the presence of TEA. These complexes show tight phosphine bite angles in the range 67.90(2)° to 74.97(4)° while the shortest belongs to tetracarbonyl chromium(0) complex **3**, the widest belongs to bis chelate nickel(0) complex **6**.

Experimental section

All air and moisture sensitive compounds were handled under an argon atmosphere using standard Schlenk techniques or in a glove box. The solvents were purified according to conventional procedures and were freshly distilled prior to use. Chemicals were obtained from Aldrich or Strem chemicals. The following spectrometers were used: Mass spectra: AMD 402. NMR spectra: Bruker AV 300 and AV 400, chemical shifts are given in ppm and are referenced to TMS or the residual non-deuterated solvent as internal standard for ^1H and ^{13}C and 85% H_3PO_4 for $^{31}P\{^1H\}$. Melting points: sealed capillary, Büchi 540 apparatus (uncorrected). – Elemental analyses: Leco Truspec Micro analyzer. Gas chromatography: HP 6890 (Hewlett Packard) chromatograph using a HP 5 column. IR: Bruker Alpha-P. Compound **1**,[6a] $Ph_2PN(^iPr)PPhCl$[7] and *fac*-$Cr(CO)_3(NCCH_3)_3$[11] were synthesized following the previously reported procedures.

$Ph_2PN(^iPr)P(Ph)NH(Et)$ (2)

$Ph_2PN(^iPr)PPhCl$ (2.0 g; 5.6 mmol) in 5 mL toluene was slowly added to a 1 : 1 mixture of $EtNH_2$ and toluene (20 mL each) at

–20 °C. The resultant turbid solution was stirred for 2 h while slowly bringing to room temperature. Volatiles were removed under vacuum and the product was extracted with n-hexane. Recrystallization from n-hexane at –40 °C furnished 1.21 g (55%) of colorless crystals of the desired product. mp 96 °C. ^{1}H NMR (C_6D_6): δ 0.97 (t, 3 H, CH_2CH_3), 1.26 (d, 6 H, $CHCH_3$), 2.34 (m, NH), 2.88 (m, 2 H, CH_2), 3.50 (m, CH), 7.02–7.68 (m, C_6H_5); ^{13}C{^{1}H} NMR ($CDCl_3$): δ 18.5 (d, J = 9.8 Hz, CH_2CH_3), 25.0–25.4 (m, $CHCH_3$), 40.8 (d, J = 28.2 Hz, CH_2), 50.0 (dd, J = 4.5, 14.8 Hz, *C*H), 127.8, 128.9–128.3 (4 signals) 128.7, 130.6, 132.7, 133.1, 139.5, 141.1, 144.2 (C_6H_5); ^{31}P{^{1}H} NMR (C_6D_6): δ 41.0 (s, br), 72.6 (s, br). Anal. Calcd for $C_{23}H_{28}N_2P_2$: C 70.04; H 7.16; N 7.10. Found: C 69.63; H 7.06; N 6.52.

[Cr(CO)$_4${Ph$_2$PN(^{i}Pr)P(Ph)NH(^{i}Pr)-*P*,*P*′}] (3)

$Cr(CO)_6$ (175 mg, 0.8 mmol) was added to a solution of $Ph_2PN(^iPr)P(Ph)NH(^iPr)$ (306 mg, 0.75 mmol) in 20 mL toluene and the resulting solution was stirred at reflux temperature for 48 h. Subsequently, the formed yellow solution was cooled down to 0 °C and filtered. Toluene was removed and the product was extracted with dichloromethane. Removal of dichloromethane under reduced pressure gave 258 mg (60%) of the greenish yellow complex. m.p. 194 °C. IR (CH_2Cl_2): ν (C≡O) 1870, 1896, 1918, 2005 cm^{-1}. ^{1}H NMR ($CDCl_3$): δ 0.58 (d, J = 6.7 Hz, 3 H, $CHCH_3$), 1.10 (d, J = 6.7 Hz, 3 H, $CHCH_3$), 1.33 (d, J = 6.3 Hz, 3 H, $CHCH_3$), 1.39 (d, J = 6.5 Hz, 3 H, $CHCH_3$), 2.56 (m, N*H*), 3.54 (m, C*H*), 4.03 (m, C*H*), 7.31–7.83 (m, C_6H_5); ^{13}C {^{1}H} NMR ($CDCl_3$): δ 24.4 (br s, $CHCH_3$) 26.2 (d, J = 4.5 Hz, $CHCH_3$), 26.8 (d, J = 4.5 Hz, $CHCH_3$), 47.6 (d, J = 11.8 Hz, CH), 54.9 (t, J = 6.4 Hz, CH), 128.3, 128.5 128.7 (mC_6H_5), 129.9, 130.2, 131.2 (pC_6H_5), 130.5, 130.7, 133.3 (oC_6H_5), 136.2, 138.2, 141.0 (iC_6H_5), 222.9, 223.7, 228.5, 228.5 (*C*O); ^{31}P{^{1}H} NMR ($CDCl_3$): δ 101.97 (d, J = 43.0 Hz), 121.06 (d, J = 43.0 Hz). HRMS (ESI): *m*/*z*: calcd for $C_{28}H_{30}CrN_2O_4P_2$: 572.1081 [M]$^+$; found: 572.1083. Anal. Calcd for $C_{28}H_{30}CrN_2O_4P_2$: C 58.74; H 5.28; N 4.89. Found: C 58.52; H 5.06; N 4.65.

[Cr(CO)$_4${Ph$_2$PN(^{i}Pr)P(Ph)NH(Et)-*P*,*P*′}] (4)

The complex **4** was prepared by following the above mentioned procedure of complex **3** using $Cr(CO)_6$ (175 mg, 0.8 mmol) and **2** (295 mg, 0.75 mmol); isolated yield: 230 mg (55%). m.p. 182 °C; IR (CH_2Cl_2): ν(C≡O) 1877, 1890, 1917, 2005 cm^{-1}. ^{1}H NMR ($CDCl_3$): δ 0.81 (d, J = 6.8 Hz, 3 H, $CHCH_3$), 1.17 (d, J = 6.8 Hz, 3 H, $CHCH_3$), 1.43 (t, J = 7.1 Hz, CH_2CH_3), 2.84 (m, NH), 3.38 (m, 1 H, $CHCH_3$), 3.59 (m, 2 H, CH_2CH_3), 7.44–7.90 (m, C_6H_5); ^{13}C {^{1}H} NMR ($CDCl_3$): δ 17.9 (d, J = 7.8 Hz, CH_2CH_3), 24.0 ($CHCH_3$), 24.2 ($CHCH_3$), 39.6 (d, J = 5.8 Hz, CH_2), 54.7 (t, J = 6.5 Hz, CH), 128.3 128.4 128.6 (mC_6H_5), 130.2 (2 signals) 130.8 (pC_6H_5), 130.3 131.4 132.4 (oC_6H_5), 136.9 137.5 139.6 (iC_6H_5), 222.2 (d,d) 224.4 228.2 (m) 228.5 (m) (CO); ^{31}P{^{1}H} NMR ($CDCl_3$): δ 101.4 (d, J = 46.0 Hz), 122.6 (d, J = 46.0 Hz). Anal. Calcd for $C_{27}H_{28}CrN_2O_4P_2$: C 58.07; H 5.05; N 5.02. Found: C 58.01; H 5.07; N 4.93.

[Cr(CO)$_3$(NCCH$_3$){Ph$_2$PN(^{i}Pr)P(Ph)NH(^{i}Pr)-*P*,*P*′}] (5)

A suspension of *fac*-$Cr(CO)_3(NCCH_3)_3$ (1.0 g, 3.86 mmol) and **1** (1.6 g, 3.91 mmol) in acetonitrile (30 mL) was stirred at 60 °C for 24 h. Then the insolubles were filtered off and the filtrate was stored at –20 °C to furnish 1.8 g (80%) of yellow crystals of complex **5**. m.p. 178 °C (decomposed); IR (nujol, cm^{-1}): ν(C≡O) 1910, 1815, 1780; IR (CH_3CN, cm^{-1}): ν(C≡O) 1923, 1830, 1802. **Major isomer**: ^{1}H NMR (CD_2Cl_2): δ 0.82 (d, J = 6.8 Hz, 3 H, $CHCH_3$), 1.03 (d, J = 6.8 Hz, 3 H, $CHCH_3$), 1.19 (t, J = 2.1 Hz, 3 H, CH_3CN), 1.25 (d, J = 6.4 Hz, 3 H, $CHCH_3$), 1.35 (d, J = 6.4 Hz, 3 H, $CHCH_3$), 2.58 (m, N*H*), 3.71 (m, C*H*, merged with minor isomer), 4.12 (m, C*H*), 7.26–8.03 (m, C_6H_5 major and minor isomer); ^{31}P{^{1}H} NMR (CD_3CN): δ 98.3 (d, J = 16.7 Hz), 119.5 (d, J = 16.7 Hz); ^{31}P{^{1}H} NMR (CD_2Cl_2): δ 99.4 (d, J = 16.7 Hz), 121.7 (d, J = 16.7 Hz). **Minor isomer**: ^{1}H NMR (CD_2Cl_2): δ 0.38 (d, J = 6.7 Hz, 3 H, $CHCH_3$), 1.12 (d, J = 6.7 Hz, 3 H, $CHCH_3$), 1.29 (dd, J = 1.3, 6.3 Hz, 6 H, $CHCH_3$), 1.41 (t, J = 2.0 Hz, 3 H, CH_3CN), 2.75 (m, N*H*), 3.51 (m, C*H*), 3.71 (m, C*H*, merged with major isomer), 7.26–8.03 (m, C_6H_5 major and minor isomer); ^{31}P{^{1}H} NMR (CD_3CN): δ 104.7 (d, J = 25.6 Hz), 118.0 (d, J = 25.6 Hz); ^{31}P{^{1}H} NMR (CD_2Cl_2): δ 107.0 (d, J = 25.6 Hz), 120.6 (d, J = 25.6 Hz). Anal. Calcd for $C_{29}H_{33}CrN_3O_3P_2$: C 59.49; H 5.68; N 7.18. Found: C 59.73; H 5.86; N 7.01.

[Ni{Ph$_2$PN(^{i}Pr)P(Ph)NH(^{i}Pr)-*P*,*P*′}$_2$] (6)

A flask was charged with of $Ni(COD)_2$ (138 mg, 0.5 mmol) and **1** (408 mg, 1.0 mmol). To this n-hexane (10 mL) was added. The slurry was stirred for 6 h at room temperature and then the formed reddish brown solution was filtered. The volume of the filtrate was reduced to 3 mL. Crystallization at –40 °C furnished 220 mg (50%) of the desired complex. m.p. 206 °C. **Major isomer**: ^{1}H NMR (THF-d_8): δ 0.03 (d, J = 6.6 Hz, 3 H, $CHCH_3$), 0.17 (d, J = 6.6 Hz, 3 H, $CHCH_3$), 0.46 (d, J = 6.2 Hz, 3 H, $CHCH_3$), 0.55 (d, J = 6.6 Hz, 3 H, $CHCH_3$), 0.86 (t, J = 6.6 Hz, 6 H, $CHCH_3$), 0.98 (d, J = 6.2 Hz, 3 H, $CHCH_3$), 1.02 (d, J = 6.6 Hz, 3 H, $CHCH_3$), 2.89 (m, 2 N*H*), 3.12 (m, 2 C*H*), 3.34 (m, C*H*), 3.68 (m, C*H*), 6.70–7.92 (m, C_6H_5);^{31}P{^{1}H} NMR (THF-d_8): 76.5–78.5 (m), 97.6–99.4 (m). Anal. Calcd for $C_{48}H_{60}N_4NiP_4$·0.5 hexane: C 66.68; H 7.35; N 6.10. Found: C 66.87; H 6.48; N 6.53 (no better analysis could be obtained even from the crystalline material).

[NiCl$_2${Ph$_2$PN(^{i}Pr)P(Ph)NH(^{i}Pr)-*P*,*P*′}] (7)

[$NiCl_2$(DME)] (135 mg, 0.613 mmol) was added to a solution of **1** (250 mg, 0.613 mmol) in THF (10 mL) at room temperature. The mixture was stirred for 16 h, then the volatiles were removed under reduced pressure. The residue was dissolved in CH_2Cl_2 and over layered with diethyl ether to give 280 mg (85%) of pure orange micro crystalline product. m.p. 270 °C (decomposed). ^{1}H NMR (CD_2Cl_2): δ 0.57 (d, J = 6.8 Hz, 3 H, CH_3), 0.89 (d, J = 6.8 Hz, 3 H, CH_3), 1.30 (d, J = 6.4 Hz, 3 H, CH_3), 1.67 (d, J = 6.4 Hz, 3 H, CH_3), 2.63 (d br, J = 10.9 Hz, N*H*), 3.26 (m, 1 H, CH), 4.26 (m, 1 H, CH), 7.45–8.24 (m, 15 H, aryl); ^{31}P {^{1}H} NMR (CD_2Cl_2): δ 41.9 (d, $^2J_{P-P}$ = 180.5 Hz), 44.1 (d, $^2J_{P-P}$ = 180.5 Hz). HRMS (ESI): *m*/*z*: calcd for $C_{24}H_{30}Cl_2N_2NiP_2$: 535.0542 and 537.051 [M – H]$^-$; found: 535.0547 and 537.0514. Anal. Calcd for $C_{24}H_{30}Cl_2N_2NiP_2$: C 53.57; H 5.62; N 5.21. Found: C 53.56; H 5.61; N 5.14.

[PdCl$_2${Ph$_2$PN(^{i}Pr)P(Ph)NH(^{i}Pr)-*P*,*P*′}] (8)

[$PdCl_2(NCPh)_2$] (470 mg, 1.23 mmol) was added to a solution of **1** (500 mg, 1.23 mmol) in CH_2Cl_2 (10 mL) at room temperature.

The mixture was stirred for 16 h, then the volatiles were removed under reduced pressure. The residue was dissolved in CH_2Cl_2 and over layered with n-hexane to give 575 mg (80%) of pure yellow micro crystalline product. m.p. 275 °C (decomposed). ^{1}H NMR (CD_2Cl_2): δ 0.61 (d, J = 6.7 Hz, 3 H, CH_3), 1.03 (d, J = 6.7 Hz, 3 H, CH_3), 1.26 (d, J = 6.5 Hz, 3 H, CH_3), 1.50 (d, J = 6.5 Hz, 3 H, CH_3), 2.81 (dd, J = 6.4, 10.5 Hz, N*H*), 3.45 (m, 1 H, C*H*CH_3), 3.89 (m, 1 H, C*H*CH_3), 7.45–8.12 (m, 15 H, aryl); ^{31}P {^{1}H} NMR (CD_2Cl_2): δ 35.5 (d, $^2J_{P-P}$ = 21.2 Hz), 36.7 (d, $^2J_{P-P}$ = 21.2 Hz). HRMS (ESI): *m*/*z*: calcd for $C_{24}H_{30}Cl_2N_2P_2Pd$: 583.0227 and 585.02517 [M – H]$^-$; found: 583.0234 and 585.0225. Anal. Calcd for $C_{24}H_{30}Cl_2N_2P_2Pd$: C 49.21; H 5.16; N 4.78; Cl 12.10. Found: C 49.16; H 5.31; N 4.88; Cl 11.73.

[$PtBr_2${$Ph_2PN(^iPr)P(Ph)NH(^iPr)$-*P*,*P*′}] (9)

[$PtBr_2$(COD)] (284 mg, 0.613 mmol) was added to a solution of **1** (250 mg, 0.613 mmol) in CH_2Cl_2 (10 mL) at room temperature. The mixture was stirred for 16 h, then the volatiles were removed under reduced pressure. The residue was dissolved in CH_2Cl_2 and over layered with n-hexane to give 415 mg (89%) of pure colorless micro crystalline product. m.p. >285 °C. ^{1}H NMR (CD_2Cl_2): δ 0.55 (d, J = 6.7 Hz, 3 H, CH_3), 0.99 (d, J = 6.7 Hz, 3 H, CH_3), 1.26 (d, J = 6.4 Hz, 3 H, CH_3), 1.47 (d, J = 6.4 Hz, 3 H, CH_3), 2.79 (m, N*H*), 3.34 (m, 1 H, CH), 3.99 (m, 1 H, CH), 7.44–8.10 (m, 15 H, aryl); ^{31}P {^{1}H} NMR (CD_2Cl_2): δ 16.3 (d, $^2J_{PP}$ = 35.0 Hz, $^1J_{Pt-P}$ = 3660 Hz), 17.9 (d, $^2J_{PP}$ = 35.0 Hz, $^1J_{Pt-P}$ = 3402 Hz). HRMS (ESI): *m*/*z*: calcd for $C_{24}H_{30}Br_2N_2P_2Pt$: 760.9803 and 762.9805 [M – H]$^-$; found: 760.9798 and 762.981. Anal. Calcd for $C_{24}H_{30}Br_2N_2P_2Pt$: C 37.76; H 3.96; N 3.67. Found: C 37.49; H 4.01; N 3.38.

trans-[$Fe(NCCH_3)_2${$Ph_2PN(^iPr)P(Ph)NH(^iPr)$-*P*,*P*′}$_2$]($BF_4$)$_2$ (10)

An acetonitrile (10 mL) solution of [$Fe(H_2O)_6$](BF_4)$_2$ (675 mg, 2.0 mmol) was added to **1** (1.63 g, 4.0 mmol) in 20 mL acetonitrile at room temperature. The resulting red-orange solution was stirred for a further two hours and then the volume of the solvent was reduced to 10 mL under vacuum. Overlayering with 30 mL of MTBE gave 1.5 g (65%) red-orange crystals of **10**. m.p. 167 °C. ^{1}H NMR (CD_3CN): **Major isomer**: δ 0.97 (d, J = 6.7 Hz, 3 H, CHCH_3), 1.16 (d, J = 6.2 Hz, 9 H, CHCH_3), 1.22 (d, J = 6.2 Hz, 6 H, CHCH_3), 1.30 (d, J = 6.5 Hz, 3 H, CHCH_3), 1.33 (d, J = 6.7 Hz, 3 H, CHCH_3), 1.98 (s br, 6 H, CH_3CN, *merged with minor isomer*), 2.88–4.11 (m, 2 N*H*, 4 C*H*, *merged with minor isomer*), 7.20–7.88 (m, 30 H, aryl, *merged with minor isomer*); **Minor isomer**: 0.89 (d, J = 6.7 Hz, 3 H, CHCH_3), 1.03 (t, J = 6.7 Hz, 6 H, CHCH_3), 1.18 (d, J = 6.7 Hz, 3 H, CHCH_3), 1.29 (d, J = 6.7 Hz, 3 H, CHCH_3), 1.37 (d, J = 6.7 Hz, 3 H, CHCH_3), 1.44 (d, J = 6.2 Hz, 3 H, CHCH_3), 1.50 (d, J = 6.7 Hz, 3 H, CHCH_3), 1.98 (s br, 6 H, CH_3CN, *merged with major isomer*), 2.88–4.11 (m, 2 N*H*, 4 C*H*, *merged with major isomer*), 7.20–7.88 (m, 30 H, aryl, *merged with major isomer*); ^{31}P {^{1}H} NMR (CD_3CN): δ 89.2–93.9 (m), 103.0–107.8 (m). Anal. Calcd for $C_{52}H_{66}B_2F_8FeN_6P_4$: C 55.35; H 5.90; N 7.45. Found: C 55.22; H 6.01; N 7.43.

Oligomerisation of ethylene. The autoclave was heated at 150 °C under vacuum for 2 h and cooled to 65 °C under an argon atmosphere. TEA was added to a solution of the complex and the resulting solution was transferred directly (or after photolysing with UV light for 30 min) into a preheated autoclave (300 mL) under an argon atmosphere. Afterwards the autoclave was pressurized with 30 bar ethylene. During the run, a constant ethylene pressure of 30 bar was applied, and the temperature was controlled through an internal cooling spiral against the exotherm of the reaction. After the run, the autoclave was cooled to below 10 °C. After releasing the excess ethylene from the autoclave, an internal standard was added (dodecahydrotriphenylene). After quenching with 10% HCl, the organic phase was analyzed by GC, and the while solids were filtered, washed, dried, and weighed.

Hydrogenation. For a detailed description of the hydrogenation equipment used see ref. 22.

X-ray structure analysis of 2–9. Data were collected on a STOE IPDS II diffractometer using graphite-monochromated Mo-Kα radiation. The structures were solved by direct methods (SHELXS-97)[23] and refined by full-matrix least-squares techniques on F^2 (SHELXL-97).[23] XP (Bruker AXS) was used for graphical representations. For complex **3** PLATON/SQUEEZE[24] was used to remove disordered solvent.

Acknowledgements

We thank PD Dr W. Baumann and our technical and analytical staff for their help.

References

1 (*a*) I. Bachert, P. Braunstein and R. Hasselbring, *New J. Chem.*, 1996, **20**, 993; (*b*) I. Bachert, P. Braunstein, M. K. McCart, F. F. Biani, F. Lashi, P. Zanello, G. Kickelbick and U. Schubert, *J. Organomet. Chem.*, 1999, **573**, 47; (*c*) I. M. R. Zubiri, M. L. Clarke, D. F. Foster, D. J. Cole-Hamilton, A. M. Z. Slawin and J. D. Woollins, *J. Chem. Soc., Dalton Trans.*, 2001, 969.
2 J. Reedijk, *J. Chem,. Soc., Chem. Commun.*, 1996, 801.
3 (*a*) F. Durap, N. Biricik, B. Gümgüm, S. Özkar, W. H. Ang, Z. Fei and R. Scopelliti, *Polyhedron*, 2008, **27**, 196; (*b*) P. Bhattacharyya, T. Q. Ly, A. M. Z. Slawin and J. D. Woollins, *Polyhedron*, 2001, **20**, 1803.
4 M. S. Balakrishna, V. Sreemvam, S. S. Krishnamunhy, J. F. Nixon, J. C. T. R. Burckett and S. Laurent, *Coord. Chem. Rev.*, 1994, **129**, 1.
5 (*a*) B. R. Aluri, N. Peulecke, B. H. Müller, S. Peitz, A. Spannenberg, M. Hapke and U. Rosenthal, *Organometallics*, 2010, **29**, 226; (*b*) B. R. Aluri, S. Peitz, A. Wöhl, N. Peulecke, B. H. Müller, A. Spannenberg and U. Rosenthal, *Acta Cryst.*, 2009, **E65**, o404.
6 (*a*) S. Peitz, N. Peulecke, B. R. Aluri, S. Hansen, B. H. Müller, A. Spannenberg, U. Rosenthal, M. H. Al-Hazmi, F. M. Mosa, A. Wöhl and W. Müller, *Eur. J. Inorg. Chem.*, 2010, 1167; (*b*) A. Wöhl, B. H. Müller, M. Hapke, N. Peulecke, U. Rosenthal, W. Müller, F. Winkler, A. Wellenhofer, H. Bölt, P. M. Fritz, M. Al-Hazmi, V. Aliyev,. F. Mosa, (Linde AG/Sabic), WO 09/006979, 2009; (*c*) N. Peulecke, B. R. Aluri, A. Wöhl, A. Spannenberg and M. H. Al-Hazmi, *Acta Cryst.*, 2009, **E65**, o1084.
7 R. J. Cross, T. H. Green and R. Keat, *J. Chem. Soc., Dalton Trans.*, 1976, 1424.
8 L. E. Bowen, M. F. Haddow, A. G. Orpen and D. F. Wass, *Dalton Trans.*, 2007, 1160.
9 T. Agapie, M. W. Day, L. M. Henling, J. A. Labinger and J. E. Bercaw, *Organometallics*, 2006, **25**, 2733.
10 H. Gabelein and J. Ellermann, *J. Organomet. Chem.*, 1978, **156**, 389.
11 D. P. Tate, W. R. Knipple and J. M. Augl, *Inorg. Chem.*, 1962, **1**, 433.
12 R. P. K. Babu, S. S. Krishnamurthy and M. Nethaji, *J. Organomet. Chem.*, 1993, **454**, 157.
13 L. Lavanant, A. S. Rodrigues, E. Kirillov, J. F. Carpentier and R. F. Jordan, *Organometallics*, 2008, **27**, 2107.
14 P. E. Garrou, *Chem. Rev.*, 1981, **81**, 229.
15 R. P. K. Babu, S. S. Krishnamurthy and M. Nethaji, *Polyhedron*, 1996, **15**, 2689.
16 C. T. Hunt and A. L. Balch, *Inorg. Chem.*, 1981, **20**, 2267.

17 Z. Z. Zhang, J. K. Zhang, W. D. Zhang, H. P. Xi, H. Cheng and H. G. Wang, *J. Organomet. Chem.*, 1996, **515**, 1.
18 A. J. Rucklidge, D. S. McGuinness, R. P. Tooze, A. M. Z. Slawin, J. D. A. Pelletier, M. J. Hanton and P. B. Webb, *Organometallics*, 2007, **26**, 2782.
19 S. Teo, Z. Weng and T. S. A. Hor, *Organometallics*, 2008, **27**, 4188.
20 G. M. Jacobsen, R. K. Shoemaker, M. R. DuBois and D. L. DuBois, *Organometallics*, 2007, **26**, 4964.
21 D. Heller, A. H. M. de Vries, J. G. de Vries, "Catalyst Inhibition and Deactivation in Homogeneous Hydrogenation", chapter 44 in *Handbook of Homogeneous Hydrogenation, 1-3*, H. G. de Vries and C. Elsevier (eds), Wiley-VCH, 2007.
22 H.-J. Drexler, A. Preetz, T. Schmidt, D. Heller, "Kinetics of Homogeneous Hydrogenation: Measurement and Interpretation", chapter 10 in *Handbook of Homogeneous Hydrogenation, 1-3*, H. G. de Vries and C. Elsevier (eds), Wiley-VCH, 2007.
23 G. M. Sheldrick, *Acta Cryst.*, 2008, **A64**, 112.
24 A. L. Spek, *PLATON, A Multipurpose Crystallographic Tool*, Utrecht University: Utrecht, The Netherlands, 2005.

